

SHEIKH-ALI COPPER DEPOSIT, A CYPRUS-TYPE VMS DEPOSIT IN SOUTHEAST IRAN

E. Rastad^{1,*}, A. Monazami Miralipour² and M. Momenzadeh²

¹ Department of Geology, Faculty of Basic Sciences, Tarbiat Modares University, Tehran,
Islamic Republic of Iran

² Geological Survey of Iran, Tehran, Islamic Republic of Iran

Abstract

Sheikh-Ali copper deposit is located 300-km southeast of Kerman in an “ophiolitic coloured melange” complex at the southeastern part of the Zagros Crushed Zone. The rock units mainly consist of pillow basalt lavas, diabase, pelagic limestone, radiolarian chert, calcareous sandstone and graywacke of Upper Cretaceous age. These units locally have an east-west trend and are emplaced as a slice between serpentinite and other ultrabasic rocks such as dunite and harzburgite, through thrust fault contacts. The country rock which hosts directly the ore horizon is a brown to red goethitic silica horizon. The silicic ore horizon was deposited stratiformly between the pelagic limestones and embedded by the pillow basaltic lavas. Chloritic and propylitic alterations can be seen in the surrounding rocks. The geometry of ore is lenticular and the lenses are conformable with the pelagic limestones, as well as pillow basalt lavas. The mineral paragenesis mainly includes pyrite, chalcopyrite, sphalerite, specularite, silica, quartz and calcite. The ore textures are massive, laminar, colloform, disseminated and rarely veinlets are present. The silicic ore horizon is about 550 meters long and 0.7 to 8.5 meters thickness. Mean and maximum content of Cu in massive ore is about 2.5 and 4.8 percent, respectively. Maximum content of Au and Ag in massive ore is about 0.64 and 75 g/t, respectively. Geochemical studies show excellent correlation between Cu and Zn in different parts of the ore body. Furthermore, the REE patterns are similar in both the pillow basalts and the ore bodies. Geological, lithological, geochemical and ore paragenesis studies suggest that the deposit can be introduced as a *Cyprus-type (Ophiolite-hosted) VMS* deposit, resulting from submarine volcanic exhalites and fumaroles, synchronous with the formation of country rocks.

Keywords: Sheikh-Ali; Copper deposit; Cyprus-type (Ophiolite-hosted) VMS; Zagros crushed zone; Iran

Introduction

The Sheikh-Ali copper deposit is located 300 km

southeast of Kerman, 150 km southeast of Baft and 130 km east of Hadjiabad (Fig. 1). It lies at the extreme southeastern end of the Zagros Crushed Zone in an

* E-mail: rastad@modares.ac.ir

“ophiolitic coloured melange” complex [1]. The ophiolite melange complex, with a northwest- southeast trend, is parallel to the Zagros thrust fault. It extends northwestwards to Turkey and finally to the Cyprus Troodos ophiolite. The Oman ophiolites are indeed the truncated extension of the same ophiolite melange [2]. This ophiolitic melange faulted and thrust with listric faults [3].

The Sheikh-Ali deposit, Ahmadabad deposit (abandoned mine) and many ore indications such as Baghchenar, Mahestan, Dahaneh-kudjin and Razdar occur within the pelagic sediments and associated pillow basalt lavas of the ophiolite melange complex (Fig. 2).

Relicts of large volumes of slag in the mining area show that ancient mining activities were extensive in the Sheikh-Ali and Ahmadabad area [4-6].

Geology

The “ophiolitic coloured melange” complex in the east of Hadjiabad (Figs. 1 and 2) includes ultrabasic rocks (such as dunite, harzburgite and serpentinite), Paleozoic marbles, glaucophane schists (blue schists), basic to intermediate volcanic rocks and pelagic and terrestrial sedimentary rocks. In the studied area they have been shown as coloured melange and tectonic melange (Fig. 2, after [1]).

These rock units are intensively tectonized in the Sheikh Ali area and have made a tectonic melange with chaotic slices and mixture of different mentioned lithological units (Fig. 3).

In the Sheikh-Ali deposit area (Figs. 3 and 4) the outcropped rocks are basic volcanic with pillow structure, diabase, pelagic limestone, radiolarian chert, calcareous sandstone and graywacke. These rocks which are probably stratigraphically in the uppermost part of the ultramafic rocks, in the normal ophiolite sequences, are ruptured as slices due to east-west trending listric thrust faults.

The basic volcanic rocks contain spilitic basalt to andesite-basalt pillow lavas, which have a variolitic texture. These basalts, from geochemical point of view, are like oceanic floor tholeiitic type, which are extensively affected by chloritic, propylitic and occasionally sericitic alterations.

The pelagic limestones comprise pink to creamy, moderate to thin bedded micritic limestone. Microfossil evidences, such as *Globotruncana Stuarti* and *Globotruncana Conica* [7,8], indicate that the micritic limestones are Upper Cretaceous (Maestrichtian) in age. General trend of limestone beds is east-west and steep variable dips. These limestones are interbedded with

pillow lavas (Fig. 5). Abrupt changes in thickness (0.5-50 m) and lateral facies in these units are very common. Pelagic sediments such as siliceous shales and association of pelagic limestone and siliceous shale, can be seen on different scales.

Black, red to brown banded radiolarian chert beds with variable thickness (0.2-15 m) are located on the contact between pillow lava and limestone beds in many localities.

Terrestrial sediments as calcareous sandstone, siltstone and graywacke are normally interbedded with pelagic limestone (Fig. 6). These rocks vary in thickness between 10 to 40 m. There is a trace of ore-bearing horizon with a thickness of 1-2 m, 300 m north of main open pit, in these sediments.

Microscopic studies confirm the relicts of radiolarite which is diagenetically recrystallized into microquartz and chalcedony (Figs. 7a and b).

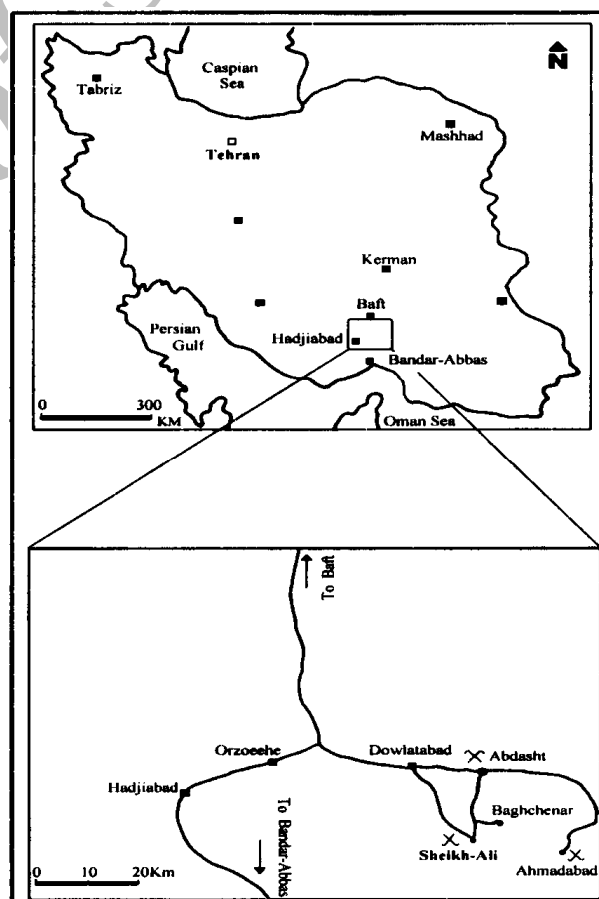


Figure 1. Geographical situation and access ways of Sheikh-Ali and Ahmadabad deposits as well as Baghchenar ore indication.

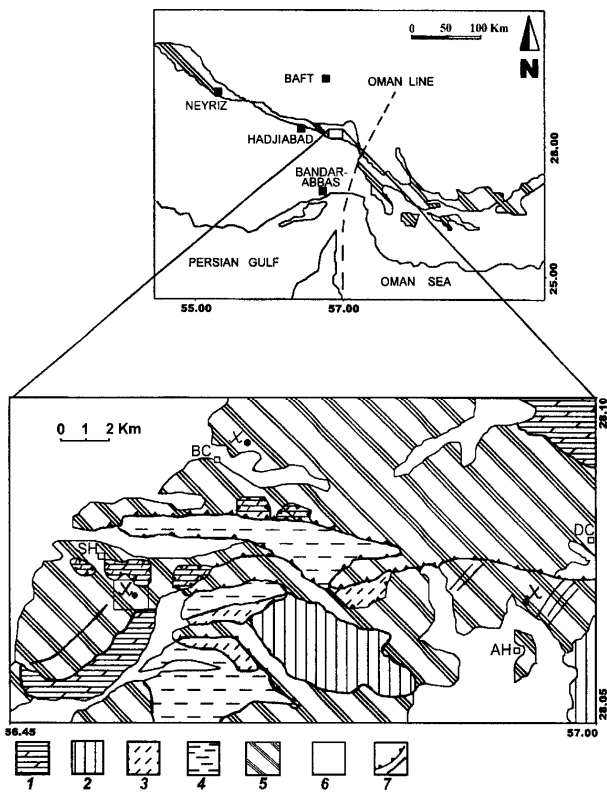
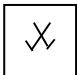
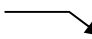


Figure 2. Situation of the studied area geological structural zones, abandoned mines and ore indications (after [1]).

- 1: Paleozoic marble
- 2: Ultramafic rocks (dunite, harzburgite)
- 3: Serpentinite
- 4: Glaucophane schist (blue schist)
- 5: Coloured melange and tectonic melange
- 6: Quaternary sediments
- 7: Thrust fault, fault

Villages:
 SH: Sheikh-Ali
 AH: Ahmadabad
 BC: Baghchenar
 RA: Razdar
 DC: Dahaneh Koudjin

X : Abandoned mine
 : Studied area

 : Ore indication

Characteristics of Silicic Ore Horizon

The country rock of the ore horizon is a brown to red goethitic silica horizon. This silicic horizon is located

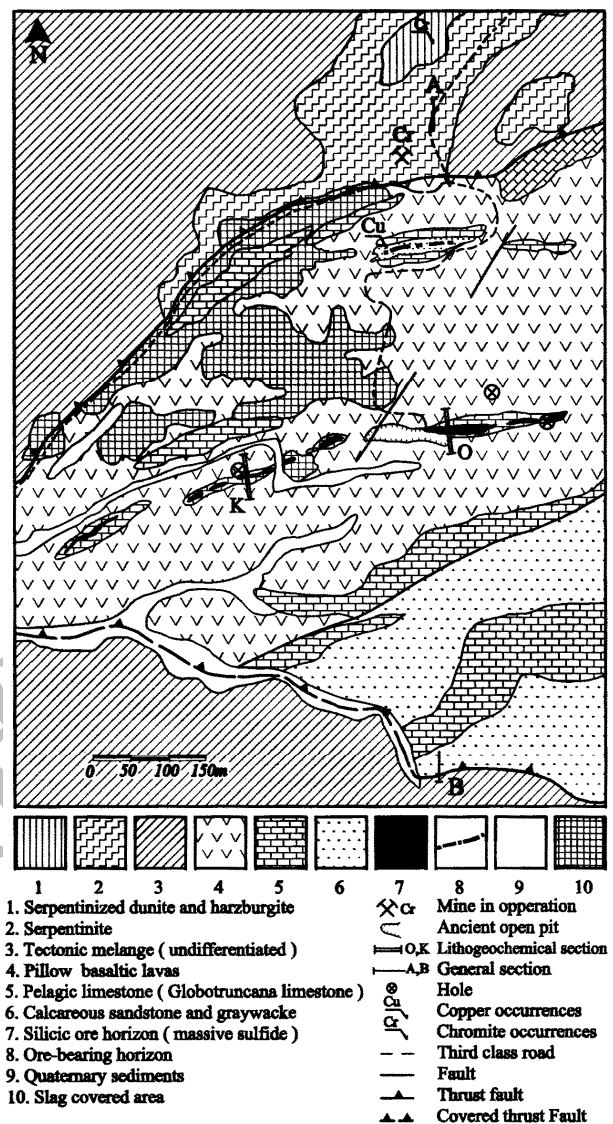


Figure 3. Geological map of Sheikh-Ali copper deposit.

stratiformly within the pelagic limestones which are in turn interlayered with pillow basaltic lavas (Figs. 4 and 5). The ore horizon is about 550 m long with an east-west direction (along pelagic limestone beds), (Fig. 8a). Congruency of the ore horizon with pelagic limestone is perfect (Fig. 8b). Ancient mining activities were run all parallel to bedding of pelagic limestones (Figs. 9a,b).

Oxidation of sulfides in the mentioned ore horizon caused dark-red to brown colors (mainly goethite). Traces of malachite and azurite on the surface and in the matrix of ore-bearing rocks are seen in some localities. Ore bodies are present as discontinuous lenses of massive sulfide. The thickness of these lenses varies from 70 cm to 8.5 m, in the main open pit trench.

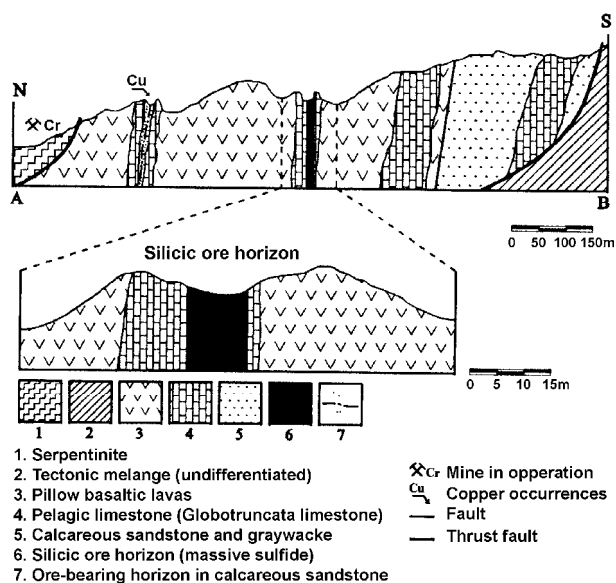


Figure 4. General section of rock units and location of the ore horizon in Sheikh-Ali deposit (For location see Fig. 3).

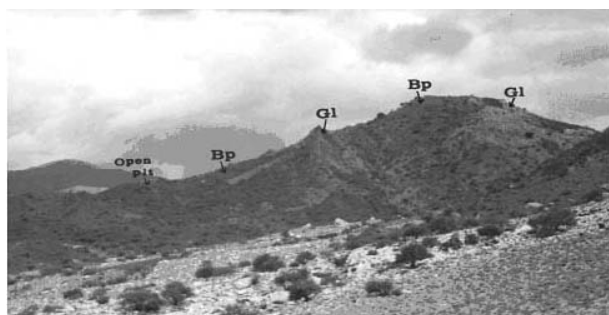


Figure 5. A general view of the rock units at Sheikh-Ali deposit; Pelagic limestones (Gl), Pillow lavas (Bp) and situation of the quarry (open pit, eastward).

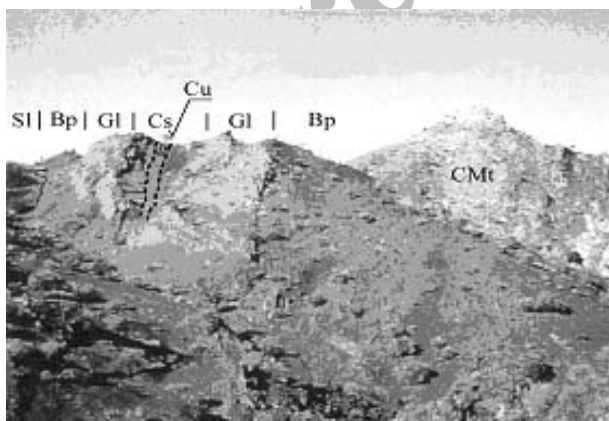


Figure 6. The location of ore-bearing calcareous sandstone and gray-wacke unit (Cs) that is embedded with pelagic limestone (Gl) and pillow basaltic lavas (Bp), (westward).

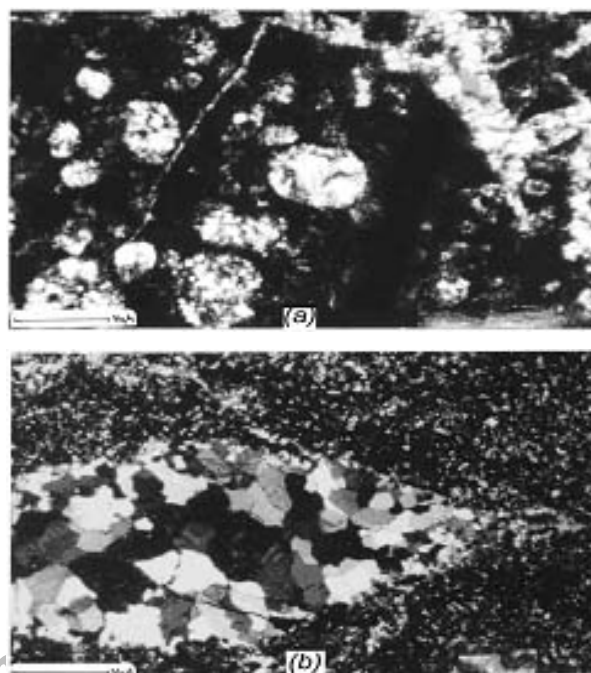


Figure 7. a) Spherical structures (probably radiolarian shells) replaced by microquartz and fibrous chalcedony (center of photo). Matrix is mainly micro to cryptocrystalline silica stained brown by iron hydroxides. b) A thin section of a chert sample, medium and coarse crystals of silica (center of photo) formed by solution and recrystallization of cryptocrystalline and amorphous silica during diagenetic processes (XPL, x250).

There is a small ore-bearing horizon in the calcareous sandstone and graywacke (Fig. 6). As mentioned before, the thickness of this ore-bearing horizon is about 1.5 m. Traces of malachite with disseminated and laminated sulfides can be seen in the sandstone. The content of Cu and Zn in this ore-bearing horizon is 0.5 and 0.21 percent, respectively.

Mean and maximum content of Cu in the silicic ore horizon is about 2.5 and 4.8 percent, respectively. Zn grades range from 0.04 to 1.24 percent and Cu/Cu + Zn ratio varies from 0.58 to 1.00. Au and Ag are not so much enriched and their maximum content in massive ore is about 0.64 and 75 g/t, respectively.

Cyprus type (Ophiolite-hosted) VMS deposits are generally poor in base- and precious metals. The richest concentrations of copper and gold were exploited from the oxidized caps. Copper grades range from 0.2 to 7.7 percent, averaging around 2 percent. Published Zn grades are generally low, and range from 0.06 to 1.2 percent, although Cu/Cu + Zn ratios vary from 0.87 to 0.16. Precious metal values vary considerably, with Ag ranging between < 5 g/t up to 69 g/t and Au from 0.1 g/t up to 2 g/t [9].

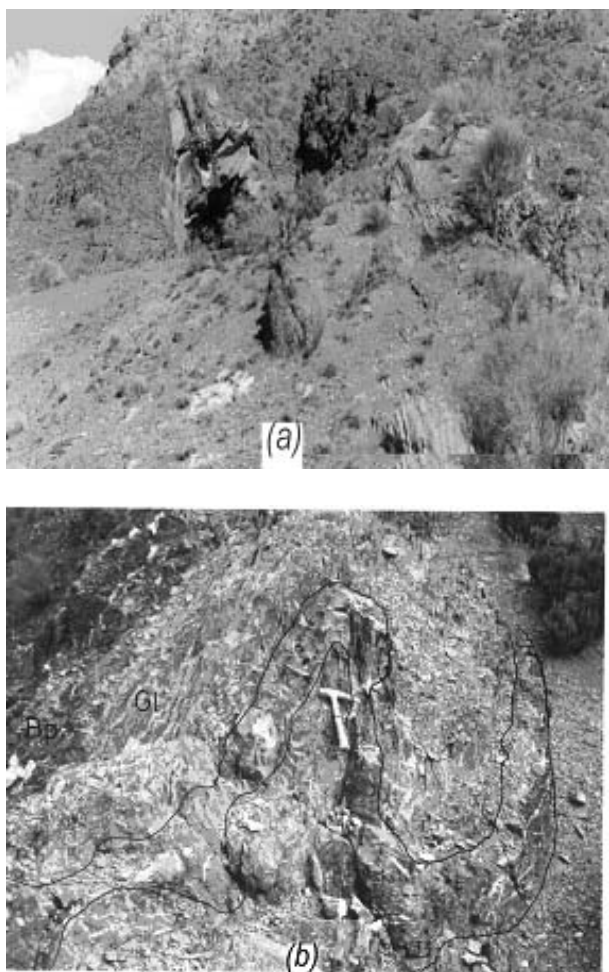


Figure 8. a) Beds of pelagic limestones (pink) embedded within the pillow lava (dark green to black). Ancient works such as quarry and holes are seen in the same strike as pelagic limestone bedding (100 m west of quarry, eastward). b) Silicic ore horizon within the cream to pink pelagic limestone layers (note the excellent congruency between the ore horizon and the interbedded folding of the pelagic limestones).

Mineralogy, Texture and Paragenesis

Ore minerals in hand specimen and on the microscopic scale show massive, laminated and colloform textures (Figs. 10, 11 and 12). Colloform ore minerals are often accompanied by jasper or cryptocrystalline silica while massive form and coarser crystals of ore minerals usually are accompanied by moderate-sized crystals of quartz and chalcedony. Ore paragenesis contains pyrite, chalcocopyrite, sphalerite, covellite, digenite, bornite, specularite and native copper.

The mineral paragenesis in the massive sulfide deposits depends on the duration and intensity of the

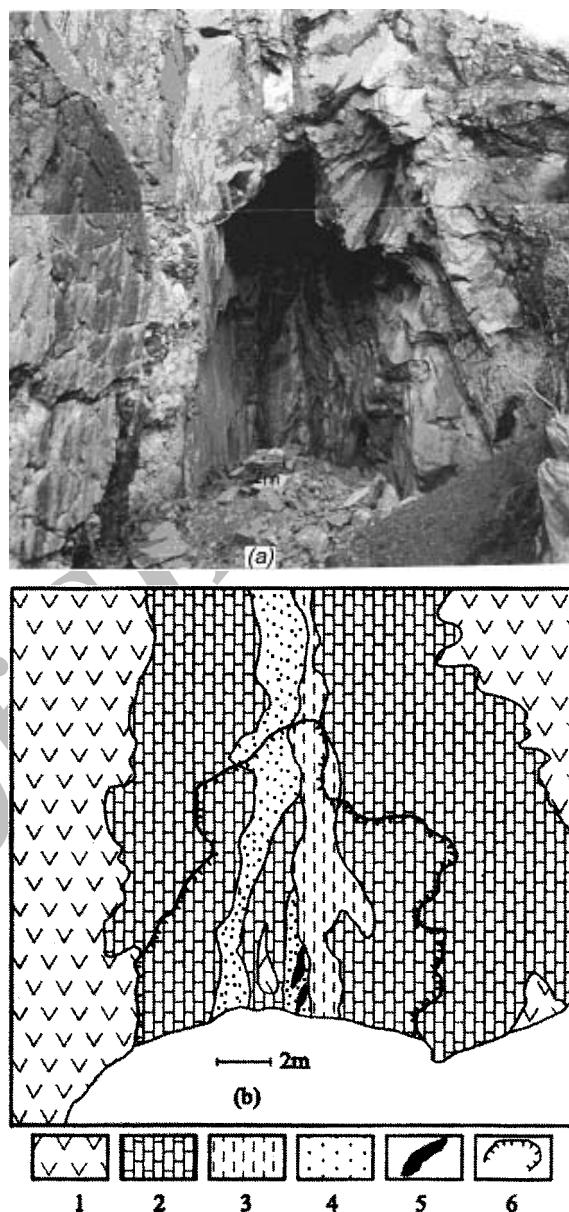


Figure 9. a) General view of eastern limit of the ancient quarry, note the relation between silicic ore horizon, lense of pelagic limestone and altered green basalts that are embedded by pelagic limestones and pillow basaltic lavas b) Scheme of Figure 9a. **1:** Pillow basaltic lavas **2:** Pelagic limestone (Globo-truncana limestone) **3:** Green basalt with high chloritic alteration **4:** Silicic ore horizon **5:** Massive sulfide lenses **6:** Quarry entrance.

underlying hydrothermal system [9]. In *Ophiolite-hosted* massive sulfide deposits pyrite is the principal sulfide mineral followed by chalcocopyrite and sphalerite. Minor amounts of hematite are also present. Quartz is the principal gangue mineral, followed by jasper [10].



Figure 10. Massive ore (dirty green) in silicic ore horizon (red to pink parts which contain malachite and azurite green and blue color, respectively) on the surface.

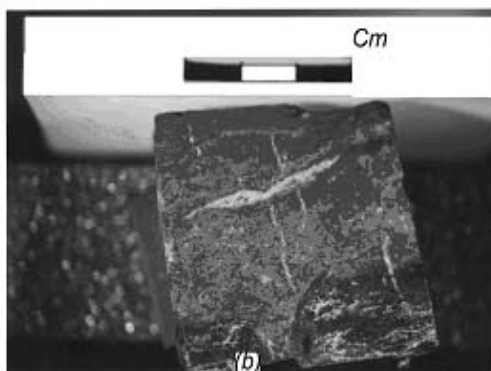
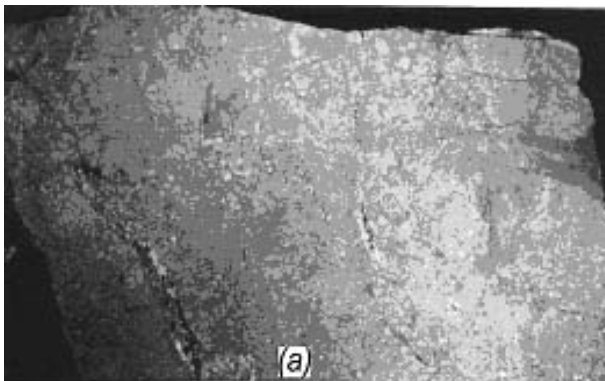


Figure 11. a) Massive ore minerals (pyrite and chalcopyrite) in hand specimen . b) Sulfide-rich silicic horizon grades into laminated ore minerals (mainly chalcopyrite) accompanied by silica (chert).

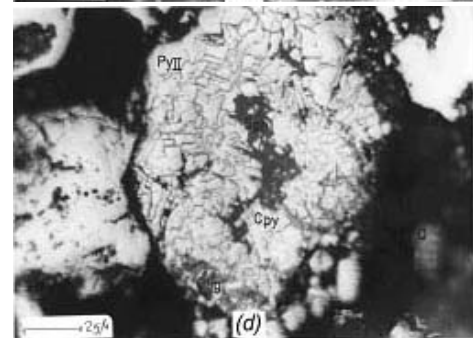
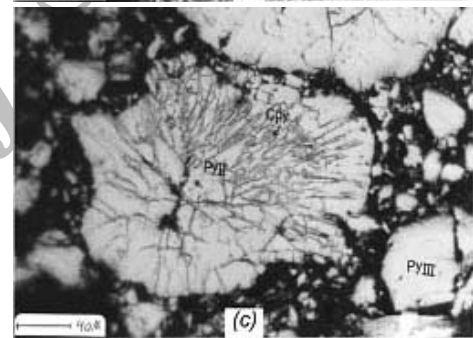
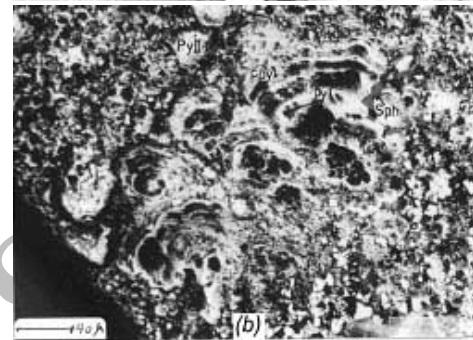
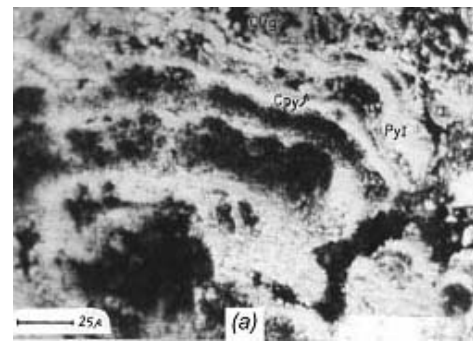


Figure 12. a) Colloform pyrite (pyrite-melnicovite), *PyI*., chalcopyrite (brassy yellow), *Cpy.*, very fine specularite (light gray), *Olig.*, cryptocrystalline silica or jasper (dark gray between colloform texture), (reflected light, PPL, oil, $\times 250$); b) Colloform(I) and subhedral(II) pyrite, sphalerite (dark gray), *Sph.*, cryptocrystalline silica or jasper (dark gray between colloform texture), (reflected light, PPL, oil, $\times 250$); c) Radial aggregate in pyrite, *PyII.*, (white to creamy), chalcopyrite (brassy yellow), (reflected light, PPL, oil, $\times 250$); d) aggregate of pyrite, *PyII.*, (white to creamy), chalcopyrite, *Cpy.*, (brassy yellow), and specularite, *Olig.*, (light gray), (reflected light, PPL, oil, $\times 400$).

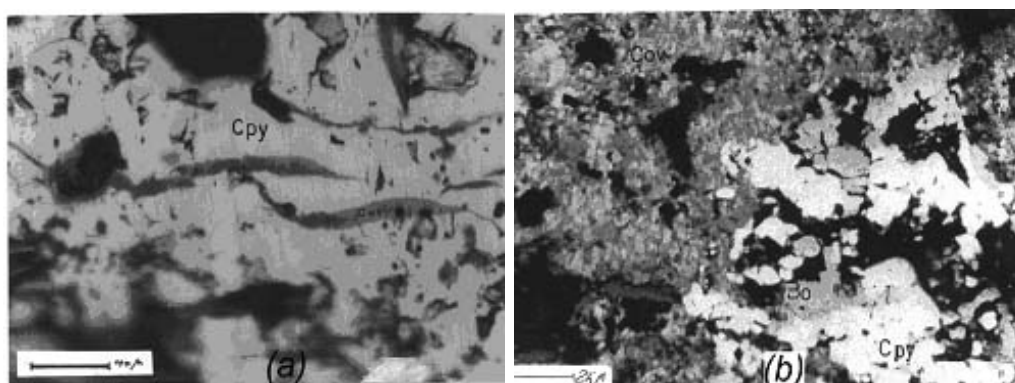


Figure 13. a) Replacement of chalcopyrite (Cpy), covellite (dark blue), digenite (light blue) in margin and fractures. b) Chalcopyrite (Cpy), bornite (Bo), covellite (Cov). (reflected light, PPL, oil, ×400).

	<i>Deposition</i>	<i>Diagenesis</i>	<i>Supergene Alteration</i>
Silica	<i>j</i>	<i>a</i> <i>b</i> <i>c</i> <i>d</i>	
Chalcopyrite	<i>c.t</i>	<i>a</i> <i>b</i> <i>i</i>	
Pyrite	<i>c.t</i>	<i>a</i> <i>b</i> <i>c</i>	
Sphalerite	<i>c.t</i>	<i>a</i> <i>b</i> <i>i</i>	
Covellite			
Digenite			
Bornite			
Specularite	<i>c.t</i>	<i>a</i> <i>b</i> <i>c</i>	
Native-Cu			
Goethite-limonite			

Figure 14. Paragenetic sequence of minerals in silicic ore horizon of Sheikh-Ali copper deposit.

a: Very fine-grained **b:** Fine to medium-grained **c:** Medium to coarse-grained
d: Very coarse-grained **i:** Inclusion **c.t:** colloform texture **j:** jasper or cryptocrystalline silica

In the Sheikh-Ali deposit pyrite is commonly fine-grained granoblastic to idiomorphic, with minor amounts of chalcopyrite and subordinate sphalerite as inclusions and fracture fillings. It is present in three forms; i.e., euhedral coarse crystals, subhedral and colloform amorphous pyrite (pyrite-melnicovite). The colloform textures contain interlayered pyrite,

chalcopyrite, sphalerite and cryptocrystalline silica (Figs. 12a and b). Chalcopyrite and sphalerite occasionally show disseminated and laminated forms but mainly fill spaces between pyrite crystals as well as replacing pyrite (Fig. 13).

According to mineralogical and ore texture studies, there are three types of colloform, fine to

medium-grained and coarse-grained sulfides and silica minerals, in the silicic ore horizon. The cryptocrystalline or jasper type of silica was formed during depositional stage. While fine to very coarse-grained quartz crystals were formed during early to late diagenesis. Sulfide minerals with colloform textures were formed syngenetically, and then extended their crystallization to fine and coarse-grained sulfides by diagenetic crystallization. Based on these studies, a paragenetic sequence is proposed (Fig. 14).

The syngenetically formation of sulfides with silica in the Sheikh-Ali copper deposit, indicate that the chemical sedimentation occurred in the early stages of sulfide deposition. Ore textures and congruency of ore minerals with rock forming minerals confirm that formation of ore and country rock, was contemporaneous during deposition and diagenesis processes (Fig. 14).

Geochemistry

Geochemical studies were accomplished by analysis of 27 samples with Neutron Activation Analysis (NAA) method for detection of 32 elements (Table 1), 21 samples with Atomic Absorption Analysis method for detection of Cu, Co and Zn (Table 2) and 14 sample for major oxides analysis (Table 3).

Mean of Cu content in basaltic rocks is about 600 g/t which is fourfold of that in oceanic floor tholeiitic basalts. Contents of Zn and Co increase but Ni often shows decrease in massive ore samples in comparison with basalts.

In order to detect genetic relationship between elements, *Cluster Analysis* performed based on computed correlation coefficient. In this case, we use *Hierarchical technique* which is the most widely applied clustering technique in the earth sciences [11]. Correlation coefficients of elements demonstrate that Cu and Zn are well correlated to each other. Dendrogram analysis of elements also confirmed high congruency of Cu, Zn and Co (Fig. 15).

Studies on the variance of ore and major elements in a general section show increasing Cu, Co, Au, As, Ag, Zn contents and decreasing V, Ni, Mn, Ca, Na contents in the ore horizon in comparison with the basaltic country rocks. Furthermore, variance of Cu, Co and Zn in four short litho-geochemical sections emphasize increasing contents of mentioned elements in all the goethitic silica horizons, as compared with basalts (Fig. 16 shows two of these sections). The profiles are perpendicular to the strike of the ore horizon.

The distribution and variance of *REE* and *Transition elements* in Sheikh-Ali pillow basalts in comparison

with standard samples indicate the affinity of these basalts to *E-type MORB* (enriched-type mid oceanic ridge basalts) (Fig. 17a). In addition, the presence of a gradual decrease in transitional element pattern (from Ti to Ni) is characteristic of *MORB* [12,13], which is observable in Figure 17b. Resemblance and coincidence of ore sample curve and pillow basalts curves are very clear and indicates confirm that the ore and the country rock were formed under the same conditions (Fig. 17b).

Discussion and Conclusions

The Sheikh-Ali copper deposit is located in a volcano-sedimentary slice of the ophiolite melange complex. The slice is restricted with two east-west trending listric faults (Figs. 2, 3 and 4).

Basaltic lavas with pillow structure, diabase, pelagic limestone, siliceous shale, banded chert, terrestrial calcareous sandstone and graywacke are the main units in the slice.

Fossils in the pelagic limestone beds indicate upper Cretaceous (Maestrichtian) age for the complex.

There is no evidence for plutonic activities near the Sheikh-Ali deposit. In addition, most of the felsic intrusive rocks in Hadjiabad 1/250,000 geological map sheet belong to the Triassic and older periods.

The country rock which hosts the ore is a brown to red goethitic silica horizon. It is well-interbedded with other sedimentary rock units. The thickness of the ore horizon changes, from 70 cm to 8.5 m, along the strike. The ore horizon was deposited between the pelagic limestones and embedded by the pillow basalt lavas.

There are three types of silica and quartz in the ore horizon. These types consist of cryptocrystalline silica, fine and coarse-grained quartz with chalcedony. The fine and coarse-grained quartz with chalcedony crystallized in diagenetic processes.

Ore geometry, in the field scale, is characterized by lensoid bodies which are conformable to the pelagic sedimentary layering. In hand specimen and microscopic scale, the ore texture is massive, laminated, disseminated, and rarely veinlets are observed.

Variolitic and microlitic textures, as well as spilitization and pillow structure of basalts indicate their speed chilling under subaqueous conditions [14,15].

Geochemical and petrogenetic studies utilizing results of *REE* analysis and various diagrams indicate that the basalts are *MORB* or *OIB* tholeiitic type.

Ore pragenesis is simple and consists of pyrite, chalcopyrite, sphalerite, covellite, bornite and native copper. The main ore minerals in the lensoid massive ore are pyrite and chalcopyrite, and the occurrence of the latter as open space filling is remarkable.

Table 1. Trace and REE element analysis of the basaltic pillow lava and ore samples from the Sheikh-Ali copper deposit

Sample No.	Lith.	Cr	Ni	Co	Sc	V	Cu	Zn	Cd	K	Rb	Cs	Ba	Sr	Ga	Ta	Hf
S9	Basalt	101	160.5	29	39.53	341	653	103	15	2324	18.75	1.245	120.8	186.8	14.25	1.99	3.96
S7	Basalt	31	141.9	26	3.86	436	750	190	19.5	1079	19.5	1.035	99	142.5	7.12	0.59	0.48
S6	Basalt	220	159.8	33	41.21	258	0.075	99	24.75	3818	17.25	1.23	129.8	187.5	12	0.41	2.4
S4	Basalt	121	162	33	38.48	323	187	98	14.25	913.1	18	1.267	117.8	187.5	16.28	0.52	2.68
S3	Basalt	136	169.5	36	42.41	335	691.5	117	1.5	498.1	17.25	1.297	124.5	210	3.09	0.57	3.44
S2	Basalt	135	136.5	27	30.31	239	616.5	61	16.5	664.1	14	1.051	107.3	172.5	20.98	0.46	1.93
G1	Basalt	291	175.5	32	36.31	244	605	91	28.5	3154	18.75	1.335	140.3	216	23.25	0.56	1.32
G2	Ore	82	45	524	65	52	12030	975	8.25	1245	15	0.825	73.5	123.8	4.28	0.42	0.35
G3	Basalt	142	192.8	79	50.93	332	710	701	13.5	332	21	1.53	135.8	233.3	16.78	0.62	2.8
E5	Basalt	346	195.8	73	32.75	201	0.23	1300	17.25	4732	25	1.53	138.8	225	19.5	0.63	2.16
E6	Basalt	220	219	86	29.75	180	0.19	1200	48	3486	21	1.2	144	200.3	16.5	0.56	1.92
E2	Basalt	344	156	45	33.05	264	0.51	705	45	4483	33	1.185	138.8	190.5	14.25	0.5	2.17
M12	Basalt	294	166.5	47	32.45	151	0.2	388	11.25	4732	22	1.32	117.8	147	14.25	0.86	1.32
M14	Basalt	314	163.5	46	39	205	767	120	15	4234	19	124.5	117.8	190.5	10.5	0.57	2.34
M23	Ore	304	34	750	94	75	18400	859	9.8	1411	20	1.305	145.5	200.3	15	1.04	2.41
M24	Basalt	370	178.5	57	44	286	4000	300	15.75	1577	20	1.41	130.5	216.8	12.75	0.71	1.85
A1	Basalt	315	170.3	35	37	225	770	135	36.75	3320	19.5	1.282	145.5	145.5	12.75	0.95	2.19
Z7	Basalt	508	156	110	28.37	219	2700	1400	24.75	9463	19	1.155	122.3	362	10.5	2.11	3.03
Z3	Basalt	245	147	37	32.33	247	750	113	18	5396	16.5	1.125	119.3	174	14.25	2.4	3.7
B14	Basalt	194	175.5	37	29.26	197	717	75	38.25	4400	20	1.32	150.8	211	10.5	1.37	2.67
A18	Basalt	227	169.5	26	27.41	209	825	88	21.75	4400	20	1.297	132.8	203.3	16.5	2.52	3.15
A11	Basalt	213	120.8	8.01	8.98	70	576	50	19.5	5894	60	3.42	117	143.3	14.81	0.84	5.86
Z4	Basalt	30	90	8	9.04	57	580.5	51	15	3901	16	0.77	325	117	21	0.52	3.43
O7	Ore	66	29	1200	85	62	39800	2300	8.1	7222	17	1.013	271	261	19.5	0.51	2.87
A45	Basalt	378	289	39	26.33	185	320	33	3.75	6200	10.5	6800	145	129.8	7.5	1.94	2.81
O10	Ore	210	20	825	210	47.8	30000	588	7.3	5800	18	0.72	120	136	14	1.4	0.425
O8	Basalt	620	342	45	26.93	171	900	113	4	2000	9.75	0.68	81.75	127.5	36	1.73	2.23

Sample No.	Lith.	Zr	Ti	Th	U	La	Ce	Nd	Sm	Eu	Gd	Tb	Dy	Ho	Tm	Yb	Lu
S9	Basalt	491.3	13908	1.69	0.585	14.5	29.34	11.79	4.63	1.35	12.73	1.45	5.6	1.838	0.12	3.8	0.82
S7	Basalt	378	3597	1.81	0.832	0.78	13.22	20.87	4.27	1.19	6.81	1.65	18.75	1.238	0.1	3.65	0.78
S6	Basalt	157	7194	0.338	0.945	6.81	18.41	6.88	3.03	0.99	3.04	1.02	4.13	1.658	0.09	3.12	0.7
S4	Basalt	500.3	12110	0.322	0.548	5.28	13.67	7.28	3.39	1.17	9.51	1.39	5.07	1.68	0.1	3.57	0.78
S3	Basalt	348	11930	0.34	0.81	5.61	13.22	7.08	3.63	1.13	9.95	1.07	5.67	0.96	0.11	3.76	0.76
S2	Basalt	431.3	5995	0.277	0.623	3.38	9.4	4.88	2.71	0.67	4.46	0.81	2.89	1.2	0.11	2.23	0.53
G1	Basalt	278	5695	0.352	1.042	2.58	5.55	5.06	1.6	0.65	2.61	0.63	3.32	1.905	0.11	2.56	0.5
G2	Ore	98	550	0.21	1.05	0.33	1.53	2.17	0.18	0.07	1.05	0.165	0.42	1.185	0.05	0.26	0.06
G3	Basalt	612	11810	0.375	0.533	2.1	2.505	3.626	1.96	0.68	7.15	0.6	3.58	1.04	0.13	3.87	0.53
E5	Basalt	558	8093	0.382	0.683	4.51	11.4	5.51	2.88	0.88	7.75	0.98	5.02	2.573	0.12	2.64	0.51
E6	Basalt	499.5	7614	0.345	1.74	5.59	12	9.98	2.95	1.04	2.23	1.03	4.06	2.513	0.13	2.41	0.6
E2	Basalt	428	8273	0.337	1.628	5.7	16.9	13.42	5.47	1.52	1.43	1.63	7.89	2.333	0.13	4.24	0.86
M12	Basalt	466.5	4976	0.337	0.473	6.01	13	5.69	2.21	0.73	8.13	0.72	2.57	1.815	0.07	1.43	0.32
M14	Basalt	493.5	8693	0.322	0.585	4.58	12.03	3.58	2.66	0.85	6.87	0.87	4.06	1.59	0.11	2.43	0.48
M23	Ore	118	425	0.58	1.85	1.5	3.5	3.14	0.95	0.8	1.2	1.05	0.71	1.19	0.14	0.28	0.49
M24	Basalt	549	5515	0.36	0.623	2.13	6.09	3.623	2.382	0.84	6.79	0.85	4.7	1.838	0.11	2.69	0.6
A1	Basalt	518	8813	0.76	1.373	7.71	17.71	8.47	2.67	0.78	2.81	0.76	4.12	1.74	0.14	2.7	0.61
Z7	Basalt	478.5	12470	2.25	0.975	19.75	36.54	15.37	3.67	1.28	5.12	0.99	4.1	1.575	0.13	2.26	0.45
Z3	Basalt	438	12829	3.11	0.473	25.62	48.4	18.55	5.08	1.12	9.34	0.263	4.09	2.055	0.13	2.69	0.57
B14	Basalt	474	11990	1.07	1.305	12.41	24.33	8.69	3.27	0.9	3.03	1.09	3.47	1.613	0.16	1.84	0.42
A18	Basalt	513.8	11870	2.29	0.878	23.75	41.23	15.47	4.68	1.24	7.77	1.12	3.74	2.325	0.12	2.16	0.46
A11	Basalt	349.5	2998	7.36	1.75	21.24	38.99	13.96	3.16	1.02	4.58	0.41	2.62	1.358	0.07	1.83	0.4
Z4	Basalt	351	2878	4.83	1.66	20.27	36.88	14.68	3.43	0.77	4.48	0.8	3.62	1.823	0.08	2.17	0.49
O7	Ore	120	450	0.81	1.84	2.15	4	4.5	2.84	0.76	2.05	0.83	0.05	1.89	0.15	0.9	0.42
A45	Basalt	171	4200	1.91	1.5	15.23	29.94	13.11	0.135	1.4	1.73	0.46	4.5	0.86	0.2	1.96	0.4
O10	Ore	88	325	0.26	2	1.2	2	3.2	0.264	0.28	0.1	0.8	0.08	1.4	0.2	0.408	0.35
O8	Basalt	87	10100	1.96	1.5	15.33	30.53	8.75	0.11	1.57	1.69	0.76	3.8	0.82	0.15	2.2	0.38

Table 2. Cu, Zn, Co, Ni, Au and Ag contents of basaltic pillow lavas and ore samples, Dis. Ore: Disseminated Ore samples, Mas. Ore: Massive Ore samples

Sample No.	Lithology	Zn (ppm)	Cu (ppm)	Co (ppm)	Ni (ppm)	Au (ppb)	Ag (ppm)	Cu / Cu + Zn
H5	Basalt	325	578	26	127	41	2	0.64
H6	Dis. Ore	2100	4800	101	18	122	9	0.70
H7	Dis. Ore	467	1700	34	17	141	17	0.78
H8	Mas. Ore	869	31500	256	19	420	34	0.97
K1	Dis. Ore	2600	3600	135	15	301	25	0.58
K2	Mas. Ore	742	36100	152	19	359	21	0.98
K3	Dis. Ore	43	7500	185	21	180	12	0.99
M31	Mas. Ore	73	48000	24	37	438	28	1.00
N1	Basalt	48	172	23	171	72	4	0.78
N2	Dis. Ore	53	8500	158	21	172	18	0.99
N9	Mas. Ore	516	43100	147	23	184	10	0.99
O2	Mas. Ore	302	36800	520	18	229	17	0.99
O5	Basalt	602	338	57	156	34	3	0.36
O6	Mas. Ore	2000	42000	266	31	180	16	0.95
O7	Mas. Ore	2300	39800	1200	29	640	75	0.76
S20	Basalt	54	187	27	164	31	3	0.78
S21	Basalt	172	417	19	173	52	3	0.70
S22	Mas. Ore	4800	16400	224	24	245	21	0.77
S23	Basalt	330	341	48	191	35	5	0.51
S24	Basalt	321	231	44	156	8	4	0.42

Table 3. Chemical analysis of major element (oxides) in basalt and diabase rocks

Sample No.	Lithology	SiO ₂	TiO ₂	Al ₂ O ₃	Fe ₂ O ₃	FeO	MnO	MgO	CaO	Na ₂ O	K ₂ O	P ₂ O ₅	H ₂ O	CO ₂
A1	Basalt	51.9	1.3	15.43	3.57	5.25	0.13	5.23	8.67	4.3	0.42	0.01	1	1.98
B14	Basalt	48.9	1.59	15.92	3.02	5.27	0.18	8.4	8.4	2.69	0.51	0.01	1	3.4
Sh11	Basalt	50.7	1.74	13.52	3.1	6.03	0.39	7.64	7.4	2.96	0.09	0	2.5	3.42
Sh12	Basalt	51.4	1.85	12.73	3.35	5.92	0.07	8.57	6.5	0.05	0.04	0.01	2	4.97
M12	Basalt	53.7	0.99	16.85	3.3	4.45	0.42	8.65	0.7	4.03	0.54	0	1	3.03
S2	Diabase	49.7	1.21	10.79	2.82	6.21	0.19	9.43	13.5	0.5	0.02	0	1	3.94
S4	Diabase	47.8	1.85	12.71	3.45	7.98	0.17	5.49	15	0.94	0.02	0	1	1.82
S6	Diabase	46.4	1.47	16.37	3.15	5.26	0.29	9.35	8.39	3.36	0.08	0	1	3.12
Z3	Basalt	49.3	2.16	16.19	2.7	3.64	0.39	5.13	7.13	5.24	0.96	0.23	1.5	3.59
M24	Basalt	51.5	1.17	14.12	4.73	6.65	0.21	5.94	7	3.5	0.11	0	1	3.04
Z7	Basalt	48.6	1.8	15.74	3.96	5.34	0.15	5.53	6.01	2.76	1.05	0.17	1	3.65
SH4	Diabase	53.8	0.3	14.2	3.04	6.83	0.19	6.5	7.06	2.25	0.51	-----	1	3.01
SH9	Basalt	52.6	0.28	15.63	1.48	6.03	0.22	7.81	9.23	1.72	0.06	-----	1.5	2.34

Alteration in the enclosing basaltic rocks mainly consists of chloritic, propylitic and lesser sericitic types.

Interpretation of geochemical data revealed that:

a) The resemblance and coincidence of distribution and variance of *transition elements* in ore and basaltic lava.

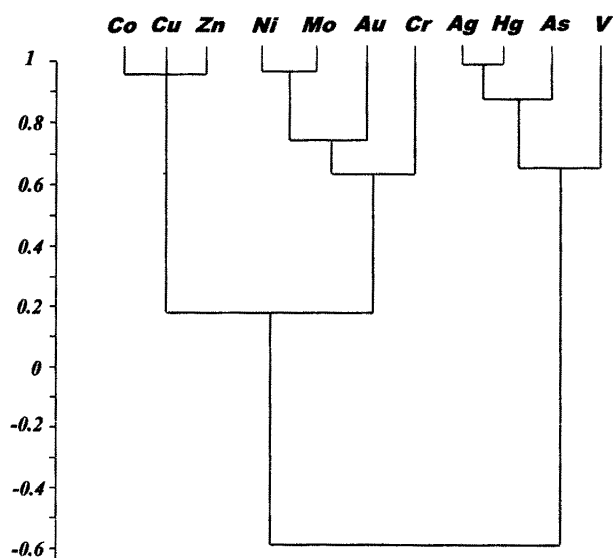


Figure 15. Dendrogram of correlation matrix, clustered by *Between groups linkage* method in Sheikh-Ali deposit.

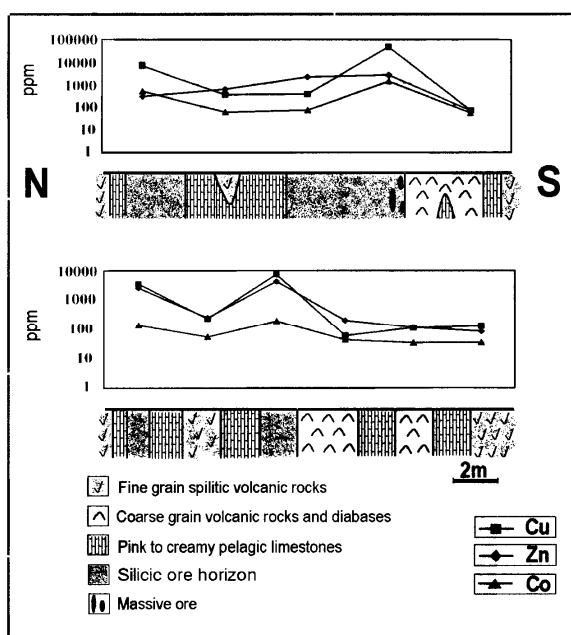


Figure 16. Variance diagram of Cu-Co-Zn in two lithochemical sections at Sheikh-Ali deposit.

b) Mean of Cu in basaltic rocks is abnormally high (about fourfold of world standard of sea floor pillow basalts contents), [16].

c) In lithochemical sections, the Cu content increases in all goethitic silica horizons. Also the element correlation diagrams confirm excellent

correlation between Cu and Zn.

The formation of *Cyprus-type (Ophiolite-hosted) VMS* deposit, is unanimously regarded as being synchronous with submarine basic activity in divergent boundaries [17-27]. Modern polymetallic massive sulfides have been found in diverse volcanic and tectonic settings on modern seafloors [10,28,29].

Studies by Skinner and Robert on S-, O- and H-isotopes resulted in presentation of the seawater sourced connate hydrothermal fluid circulation model [22,26]. On the basis of this model, fluids will ascend synchronous with or a short time after the formation of basaltic pillow lava and cause leaching and transport of the metal contents of the volcanic rocks. The low temperature of mixing seawater and reducing conditions result in sulfide deposition as soon as the connate fluids reach seawater. In this model, the source of fluids and sulfur is sea water while the tholeiitic basalts and diabasic dikes react with high temperature, low pH connated sea water and release metallic ions [30].

In *Ophiolite-hosted* deposits, in some cases, sulfide mineralization occurs within the conformably overlying sedimentary package. This type of massive sulfide deposits is known as "*Massive sulfide deposits within sedimented ophiolites*" [9]. The massive sulfide deposits in some "*Sedimented Ophiolite*" suites are hosted in higher beds of the sedimentary package within argillite/graywacke and are associated with mafic to ultramafic sills [31,32]. The Anayatak copper deposit, in the Turkish Taurides which is hosted by cretaceous ophiolites [33], is an example of the *Sedimented Ophiolite- VMS* type deposits, and the Cretaceous-Paleogene Ochiaizawa deposit in the Shimokawa mining district of Japan is another example [34].

Deposits such as those within the Turkish ophiolites, appear to have been formed in the sediments of epicontinental rift basins in which MORB basalt-covered sea floor is quickly inundated with pelagic and terrestrial sediments or within immature epicontinental or rifted arc environments. These deposits differ compositionally from the classic *Cyprus-type VMS* deposits. The latter possess more concentrations of Co and Ni.

On the basis of following evidence, we consider the Sheikh-Ali copper deposit as a *Sedimented Ophiolites of Ophiolite melange-hosted (Cyprus-type) volcanogenic massive sulfide* deposit:

- The country rock is a part of a slice of ophiolite melange, volcano-sedimentary unit and the ore horizon is conformable with basalt pillow lavas and pelagic limestone beds.

- Ore is accompanied by jasper, chalcedony and quartz.

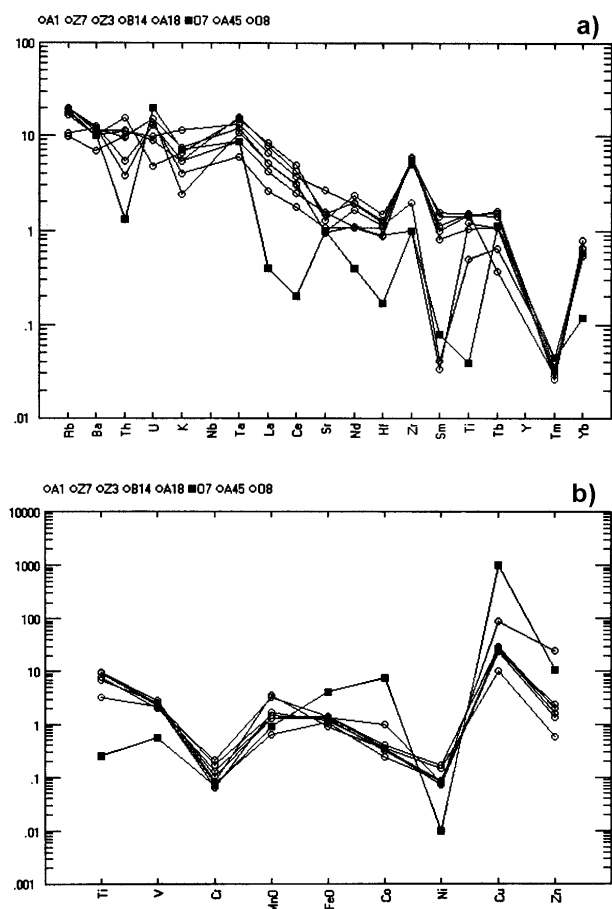


Figure 17. a) REE and trace element pattern of basalt samples normalized to MORB REE. Negative gradient in all sample curves indicates differentiation in the sampled rocks and consequently enrichment of the incompatible elements in comparison with the compatible elements. b) Transition elements pattern in ore and country rock samples normalized to *P. Mantle*; Note the excellent coincidence of the curves for ore samples and basaltic country rock samples. Fill square: ore sample, Open circles: lava samples.

– Chloritic, propylitic and sericitic alterations occur in basaltic rocks.

– Ore paragenesis consists of Cu-Zn and Fe minerals.

– Geochemical values of Cu and Zn in ore and country rocks are well correlated.

– Plutonism and related processes assumed as sources of Cu are absent in the area.

– In comparison to classic *ophiolite-hosted VMS* and *Sedimented Ophiolite VMS* deposits, it seems that the characteristics of Sheikh-Ali deposit, such as content of Cu, Zn, Au, Ag and Cu/Cu+Zn ratio and association with pelagic and terrestrial sediments, are more similar to *Sedimented Ophiolite VMS*, such as Anayatak copper deposit in Turkey.

– The extension of the ophiolitic complex beyond Iranian borders, in the northwest hosts some Cyprus-type VMS deposits in Turkey, such as Ergani, Kur, Ana Yatak,... [34-37] while in the south it hosts some others such as Lasil, Bayada,... in Oman [38]. The Ghezeldush prospect in northwest Iran near Maku [39], and the Remeshk group of ancient mines in southeast Iran [6] which are all hosted in the same ophiolite complex, show some similarities with the Sheikh-Ali deposit.

Acknowledgements

The author would like to thank anonymous reviewers for their critical suggestions. We are also grateful to the Research Council of the Tarbiat Modarres University for research grant for this work. The authors gratefully acknowledge the technical assistance given by the Geological Survey of Iran.

References

1. Sabzehei M., Alavi Tehrani N., Berberian M., Hushmandzade A., Majidi B. and Nowgol-Sadat M.A.A. 1:250000 geological map of Hadjiabad. Geological Survey of Iran (1994).
2. Boulin J. Structures in southwest Asia and evolution of the eastern Tethys. *Tectonophysics* **196**: 68-211 (1991).
3. Alavi Tehrani N. Ophiolitic rock complexes in Iran; their disputable problems and conclusions. Geological Survey of Iran. Int. report (1975).
4. Basin & Hubner. Old copper mine at Sheikh-Ali. Geological Survey of Iran. Int. report (1965).
5. Basin & Hubner. Copper deposits in Iran. Geological Survey of Iran. Report No. 13 (1969).
6. Paragon Cosultant Engineers. Report on the preliminary mining reconnaissance of Eastern Iran Project. Geological Survey of Iran, Rep. No. 198 (1978).
7. Kalantari A. Microfacies of carbonate rocks of Iran. National Iranian Oil Company, Geological laboratories publication, No. 11, 520 p. (1986).
8. Loeblic A.R. and Tappan H. *Foraminiferal Genera and Their Classification*. Van Nostrand Reinhold, New York, 1059 p. (1988).
9. Galley A.G. and Koski R.A. Setting and characteristics of Ophiolite-Hosted Volcanogenic Massive Sulfide deposits: Processes and examples in modern and ancient settings. *Reviews in Economic Geology* **8**: 221-246 (1999).
10. Herzig P.M. and Hannington M.D. Polymetallic massive sulfides at the modern seafloor, A review. *Ore Geology Reviews* **10**: 95-115 (1995).
11. Davis J.C. *Statistical and Data Analysis in Geology*. John Wiley & Sons publications, 645 p. (1986).
12. Wilson M. *Igneous Petrogenesis, A Global Tectonic Approach*. Chapman & Hall, London, 466 p. (1989).
13. Le Maitre R.W. *A Classification of Igneous Rocks and Glossary of Terms*. Blackwell, Oxford, 193 p. (1989).
14. Amstutz G.C. *Spilites and Spilitic Rocks*. Springer, Berlin, Heidelberg, New York (1974).

15. Harold L., Gibson H.L., Morton R.L. and Hudak G.J. Submarine volcanic processes, deposits and environments favorable for the location of volcanic-associated massive sulfide deposits. 5th Annual Short Course: Magmatism, Volcanism and Metallurgy, France (1998).
16. Rollinson H.R. *Using Geochemical Data, Evaluation, Presentation and Interpretation*. Longman Scientific & Technical, 353 p. (1993).
17. Govett G.J.S. and Pantazis T.M. Distribution of Cu, Zn, Ni and Co in the Troodos pillow lava series, Cyprus. *Inst. Mining Metallurgy Trans.* **80**: B27-B46 (1971).
18. Constantinou G. and Govett G.J.S. Geology, geochemistry and genesis of Cyprus sulfide deposits. *Economic Geology* **68**: 843-858 (1973).
19. Sillitoe. Environments of formation of volcanogenic massive sulfide deposits. *Economic Geology* **68**: 1321-1336 (1973).
20. Solomon M. "Volcanic" massive sulfide deposits and their host rocks, A review and an explanation. In: Wolf K.H. (Ed.), *Handbook of Strata-bound and stratiform ore deposits*. Amsterdam, Elsevier **6**: 21-50 (1976).
21. Adamides N.G. The form and environment of formation of the Kalavassos ore deposits, Cyprus. In: Panayiotou A. (Ed.), *Ophiolites. Int. Ophiolite Symp., Cyprus (1979)* 117-178 (1978).
22. Skinner B.J. Seventy-fifth Anniversary Volume of *Economic Geology* (1981).
23. Robinson P.T. and Malpas J. The Troodos Ophiolite of Cyprus, new perspective on its origin and emplacement. Cyprus Geological Survey Department Symposium "Troodos 1978", Proceedings (1987).
24. Sawkins F.J. Integrated tectonic-genetic model for volcanic-hosted massive sulfide deposits. *Geology* **18**: 1061-1064 (1990).
25. Sawkins F.J. *Metal Deposits in Relation to Plate Tectonics*. Springer Verlag, 323 p. (1990).
26. Robert R.G. and Sheahan P.A. *Ore Deposit Models*. Love Printing Service, Ltd Ottawa. Second Ed., 194 p. (1990).
27. Hall J.M. and Yung J.S. A preferred environment of preservation for volcanic massive sulfide deposits in Troodos Ophiolite (Cyprus). *Economic Geology* **89**: 851-857 (1994).
28. Scott S.D., Chese R.L., Hamington M.D., Michael P.J., McConachy T.F. and Shea G.T. Sulfide deposits, tectonics and petrogenesis of Southern Explorer Ridge, Northeast Pacific Ocean. *Int. Ophiolite Symposium, Cyprus (1987)*.
29. Scott S.D. Polymetallic massive sulfide deposits at the modern seafloor, A review. 5th annual short course: Magmatism, Volcanism and Metallurgy, France. Expanded from a manuscript entitled: "Polymetallic sulfide riches from the deep: Fact or Fallacy?" prepared for a Dehlem Conference on "Use and Misuse of the seafloor", March 17-22, 1991, Berlin (1998).
30. Juteau T. The seawater-oceanic crust interaction. 5th Annual Short Course: Magmatism, Volcanism and Metallurgy, France (1998).
31. Slack J.F. Descriptive and grade-tonnage models for Besshi-type sulfide deposits, In Kirham RV Sinclair WD Thorpe R.L. and Duke J.M. (Eds.), *Mineral deposit modelling*. Geological Association of Canada, Special Paper **40**: 343-371 (1993).
32. Zierenberg R.A., Koski R.A., Morton J.I., Bouse R.M. and Shanks W.C. Genesis of massive sulfide deposits on a sediment-covered spreading center, Escanaba Trough, Southern Gorda Ridge. *Economic Geology* **88**: 2069 (1993).
33. Griffiths W.R., Albers J.P. and Oner O. Massive sulfide copper deposits of the Ergani-Maden area, Southeastern Turkey. *Economic Geology* **67**: 701-716 (1972).
34. Mariko T. and Kato Y. Host rock geochemistry and tectonic setting of some volcanogenic massive sulfide deposits in Japan: Examples of the Shimokawa and the Hitachi Ore deposits. *Resource Geology* **44**: 353-367 (1994).
35. Bamba T. Ophiolite and related copper deposits of the Ergani mining district. *Turkey mineral resources exploration* **86**: 36-57 (1976).
36. Gagatay M.N. and Boyl D.R. Geology, geochemistry and hydrothermal alteration of Madenkoy massive sulfide deposit, eastern Black sea region, Turkey. In: Ridge J.D. (Ed.), *IAGID symposium 5th proc.* (1980).
37. Gagatay M.N. Hydrothermal alteration associated with volcanogenic massive sulfide deposits, Example from Turkey. *Economic Geology* **88**: 606-621 (1993).
38. Alabaster T., Pearce J.A., Mallick D.I.J. and Elboushi I.M. The volcanic stratigraphy and location of massive sulfide deposits in Oman Ophiolite. In: Panayiotou A. (Ed.), *Ophiolites. Int. Ophiolite Symposium, Cyprus (1979)* 751-757 (1978).
39. Emamalipour A. and Masoudi J. Introduce of Ghezeldash copper deposit as first Cyprus-type massive sulfide deposit in Khoy-Maku ophiolite melange. First annual symposium of Geological Society of Iran (1995).